Solid State Ionics 192 (2011) 42–48

Contents lists available at ScienceDirect

Solid State Ionics

journal homepage: www.elsevier.com/locate/ssi

Oxygen deficiency, vacancy clustering and ionic transport in $(La,Sr)CoO_{3-\delta}$

E.V. Tsipis [a], E.N. Naumovich [b], M.V. Patrakeev [c], A.A. Yaremchenko [b], I.P. Marozau [b], A.V. Kovalevsky [b,d], J.C. Waerenborgh [a], V.V. Kharton [b,*]

[a] Chemistry Department, Instituto Tecnológico e Nuclear, CFMC-UL, EN 10, 2686-953 Sacavém, Portugal
[b] Department of Ceramics and Glass Engineering, CICECO, University of Aveiro, 3810-193 Aveiro, Portugal
[c] Institute of Solid State Chemistry, Ural Division of RAS, 91 Pervomayskaya Str., Ekaterinburg 620219, Russia
[d] Conversion and Separation Technology, Flemish Institute for Technological Research (VITO), 2400 Mol, Belgium

ARTICLE INFO

Article history:
Received 23 August 2009
Accepted 22 March 2010
Available online 30 April 2010

Keywords:
Lanthanum–strontium cobaltites
Oxygen nonstoichiometry
$p(O_2)$–T–δ diagrams
Ionic transport
Vacancy clustering
Mössbauer spectroscopy

ABSTRACT

The equilibrium $p(O_2)$–T–δ diagrams of perovskite-type $La_{1-x}Sr_xCoO_{3-\delta}$ ($x=0.3$–0.7), collected at 873–1223 K in the oxygen partial pressure range 10^{-5}–1 atm by coulometric titration and thermogravimetric analysis, were analyzed in order to appraise the effects of the point-defect interactions. The nonstoichiometry variations were adequately described combining the rigid-band approach for delocalized holes and the pair-cluster formation reaction involving oxygen vacancies and Co^{2+} cations, whilst coulombic repulsion between the positively charged vacancies can be neglected. The resultant relationships between the oxygen chemical potential and mobile vacancy concentration were used for numerical regression analysis of the steady-state oxygen permeation through dense $La_{1-x}Sr_xCoO_{3-\delta}$ membranes, affected by the surface exchange kinetics when Sr^{2+} content is higher than 40–50%. The calculated ionic conductivity is strongly influenced by the defect association processes, and decreases with decreasing concentration of the mobile vacancies as clustering starts to prevail on reduction. The Mössbauer spectroscopy studies of $La_{1-x}Sr_xCoO_{3-\delta}$, doped with 1 mol% ^{57}Fe isotope and moderately reduced at $p(O_2)\approx10^{-5}$ atm, show no long-range vacancy ordering at $x\leq0.5$.

1. Introduction

Lanthanum–strontium cobaltites with ABO_3 perovskite-type structure, $(La,Sr)CoO_{3-\delta}$, possess very high levels of p-type electronic conduction, oxygen ion diffusivity, oxygen surface exchange rates and electrocatalytic activity in the reactions involving oxygen [1–10]. These properties, attracting great interest to the cobaltite-based systems for a variety of high- and low-temperature electrochemical applications, are all dependent of the oxygen stoichiometry and oxygen thermodynamics. Moderate additions of Sr^{2+} in $La_{1-x}Sr_xCoO_{3-\delta}$ result in increasing hole concentration and delocalization, leading to maximum electronic transport at $x\approx0.3$–0.4. On further Sr^{2+} doping, the charge compensation mechanism via the oxygen vacancy formation starts to prevail; the partial ionic conductivity increases with strontium content up to $x\approx0.7$, and then exhibits a decrease due to extensive ordering processes in the oxygen sublattice and phase separation [1,6–8,10]. Although some aspects in $(La,Sr)CoO_{3-\delta}$ behavior can be successfully represented by the standard point-defect models (*e.g.* [10,11]), the essentially itinerant nature of p-type electronic charge carriers requires to avoid use of the ideal solution-based approaches for description of the cobalt sublattice. The oxygen nonstoichiometry in $(La,Sr)CoO_{3-\delta}$ is often analyzed using a simplified rigid-band approach assuming that oxygen release from the perovskite lattice results in gradual filling of the electronic states in a wide band, rising the Fermi level, whilst any non-idealities in the oxygen sublattice are neglected [3,4]. At the same time, numerous experimental data (see [7,8,12,13] and references therein) indicate a significant role of short- and long-range ordering processes in the oxygen sublattice, particularly at $x>0.5$ and moderate oxygen chemical potentials.

The major purpose of this work was to evaluate effects of defect clustering phenomena in $La_{1-x}Sr_xCoO_{3-\delta}$ ($x=0.3$–0.7) on the oxygen deficiency variations and ionic transport, using the rigid-band model [3] for p-type electronic charge carriers. As the analysis of point-defect interactions leads to complex statistical models and, hence, requires large arrays of experimental data points, the equilibrium $p(O_2)$–T–δ diagrams of lanthanum–strontium cobaltites were collected in wide ranges of temperature and oxygen partial pressure by thermogravimetric analysis (TGA) and coulometric titration (CT). The obtained parameters describing behavior of the perovskite lattice components were then used to model steady-state oxygen permeation through dense cobaltite membranes. The local structural features associated with vacancy ordering were also evaluated by Mössbauer spectroscopy (MS) of $(La,Sr)CoO_{3-\delta}$ doped with 1 mol% ^{57}Fe, where the isotope probe was selected close to possible minimum in order to minimize strains and structural changes in the host cobaltite matrix.

* Corresponding author. Tel.: +351 234 370263; fax: +351 234 425300.
E-mail address: kharton@ua.pt (V.V. Kharton).

0167-2738/$ – see front matter © 2010 Elsevier B.V. All rights reserved.
doi:10.1016/j.ssi.2010.03.029

2. Experimental

Single-phase ceramics of $La_{1-x}Sr_xCoO_{3-\delta}$ ($x=0.3$, 05 and 0.7) with >93% density were prepared via the glycine-nitrate synthesis route, calcination at 1073–1273 K, ball-milling, pressing at 180–250 MPa and final sintering in air at 1520–1650 K for 2 h. The powdered samples used for X-ray diffraction (XRD), CT and TGA were obtained by grinding of sintered ceramics. XRD showed the formation of single perovskite-type phases with rhombohedral ($x=0.3$ and 0.5) or cubic ($x=0.7$) structure. The overall cation composition was confirmed by the inductively-coupled plasma (ICP) spectroscopic analysis. The equipment and procedures used for materials characterization, including the oxygen permeation and total conductivity measurements, were described elsewhere ([5,8,11,14–16] and references cited). TGA was carried out in the regimes of temperature cycling at 293–1323 K and isothermal dwells at 873–1223 K in flowing dry air, with subsequent reduction in 10%H_2–90%N_2 mixture at 1373 K. The calculated values of total oxygen content (3–δ) at atmospheric oxygen pressure were used as the reference points for the CT data arrays. The average reproducibility error of the δ values at 873–1223 K, estimated from 10 measurement cycles, was lower than ± 0.004 atoms per formula unit. One example illustrating reproducibility of the TGA data is presented in Fig. 1A. The CT measurements were performed in isothermal regime, varying $p(O_2)$ in the range 10^{-5} to 1 atm, at 873–1223 K. An excellent reproducibility validated after each redox cycle, as illustrated by Fig. 1B, confirmed zero leakage in the coulometric titration cells. The same conclusion was drawn comparing the oxygen nonstoichiometry variations at atmospheric $p(O_2)$, measured by the TGA and CT methods. For the Mössbauer spectroscopy studies a series of ^{57}Fe-doped compositions, $La_{1-x}Sr_xCo_{0.99}Fe_{0.01}O_{3-\delta}$ ($x=0.3$, 05 and 0.7), was synthesized under conditions identical to those for the iron-free materials. After XRD, the samples were annealed in air or in flowing argon at 973–1223 K for 10 h, and then slowly cooled or quenched in liquid nitrogen. The Mössbauer spectra were collected at 4 and 290 K on a transmission constant-acceleration spectrometer with a ^{57}Co (Rh) source as described elsewhere [14,15], and analyzed using MossWinn software [17]. For all MS data, isomer shifts (IS) are given relative to metallic α-Fe at room temperature.

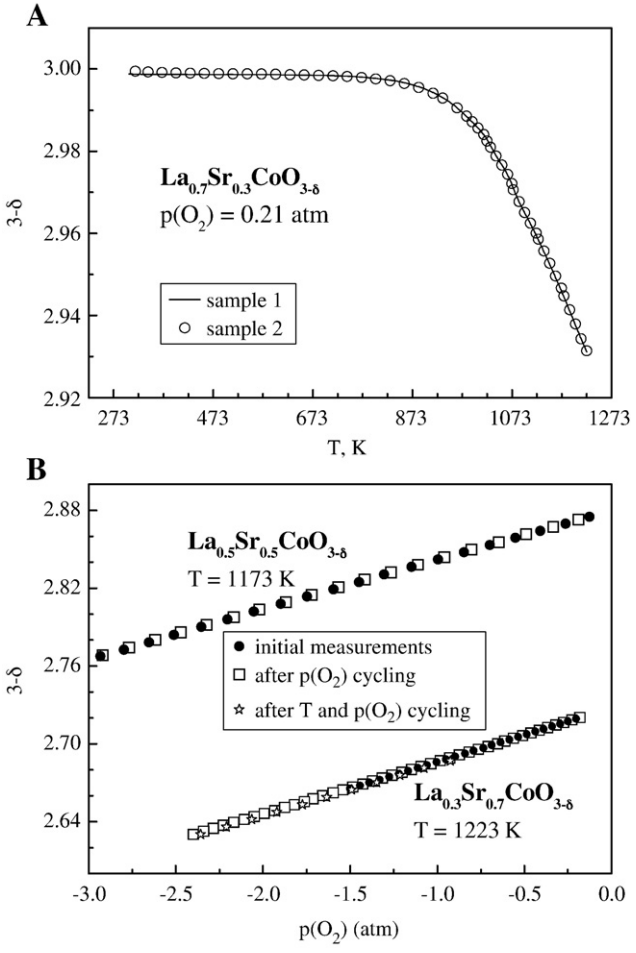

Fig. 1. Reproducibility of the oxygen content variations measured by TGA (A) and coulometric titration (B).

3. Results and discussion

3.1. Oxygen nonstoichiometry

In this work, all statistical-thermodynamic models for the equilibrium $p(O_2)$–T–δ diagrams (Fig. 2) included the hole contribution, described in framework of the rigid-band approach [3] and formulated as:

$$\mu(h) = \mu\left(h^0\right) + \frac{\left[h^{\bullet}\right]-\left[h^0\right]}{g(\mu(h^0))} \tag{1}$$

where μ is the chemical potential consisting of concentration-dependent (μ') and concentration-independent (μ^0) parts, $[h^0]$ is the electron-hole concentration at zero δ, and $g(\mu(h^0))$ is the electronic density of states at the Fermi level. Hereafter, the Kröger–Vink notation is used and all concentration-related terms are normalized to one formula unit. If the generation of p-type charge carriers is significantly contributed by intrinsic electronic disordering when Co_B' exists predominantly in the form of any clusters with oxygen vacancies, such as $\langle V_O - Co_B\rangle^{\bullet}$, the parameter $[h^0]$ is equal to $[Sr_A']$. The concentration-dependent part of the vacancy chemical potential can be generally formulated as

$$\mu'(V_O^{\bullet\bullet}) = RT\ln\frac{\left[V_O^{\bullet\bullet}\right]}{N(\delta)-\delta} \tag{2}$$

where $[V_O^{\bullet\bullet}]$ is the concentration of mobile oxygen vacancies, δ is the total concentration of vacant oxygen sites measured by TGA and CT, and $N(\delta)$ is the corresponding number of states. In the simplest case when all oxygen sites are energetically equivalent and vacancies interaction can be neglected (Model 1), the latter quantity is equal to the number of oxygen sites: $N(\delta)=[O_O^{\Sigma}]=3$. When the site-exclusion effects caused by coulombic repulsion between the vacancies are significant (Model 2), $N(\delta)$ is determined by the probability of complete occupation of n neighboring oxygen sites:

$$N(\delta) = \left[O_O^{\Sigma}\right]\left(1-\frac{\delta}{\left[O_O^{\Sigma}\right]}\right)^n. \tag{3}$$

If no vacancy can be located in the first coordination sphere near a vacant site, $n=8$.

Preliminary analysis of the $p(O_2)$–T–δ diagrams (Fig. 2) demonstrated that, since the average oxidation state of cobalt cations at relatively low $p(O_2)$ and elevated temperatures becomes quite close to 3+, the electron-hole equilibrium and Co_B' formation cannot be neglected. For Models 1 and 2, the latter species were considered as polarons localized near oxygen vacancies, forming stable pair clusters $\langle V_O - Co_B\rangle^{\bullet}$:

$$\mu'\left(\langle V_O - Co_B\rangle^{\bullet}\right) = RT\ln\frac{\left[\langle V_O - Co_B\rangle^{\bullet}\right]}{N(\delta)-\delta}. \tag{4}$$